Volume 4, Number 2 | ISSN 2331-4621

THE FINGER LAKES JOURNAL OF SECONDARY SCIENCE

Edited by the New Visions Engineering Students at the Tompkins-Seneca-Tioga BOCES Career and Technical Education Center

David M. Syracuse, Principal Editor

www.fljss.com

TABLE OF CONTENTS

Editor's Note

The push for a more integrated, "STEAM-themed" science curriculum, is, in general a good thing. It aligns K-12 education with the "real world," in which concepts and knowledge are not bunched up into silos and hidden away from each other; rather, they're allowed to organically merge and flow as dictated by the problem at hand. Although I don't have any evidence to support my guess, I suspect that even the most capable students that pass through our classes come out in the real world wondering why chemistry was kept so far away from earth science. Or why physics and math *and music* weren't woven together into one colorful tapestry of learning. The answer that you get depends on to whom you pose the question.

Ask a teacher, and you'll hear that there is a test that the students must pass at the end of the year, in order to ensure that they have a good general foundation of knowledge in that particular subject area. And because there is this test, in, say, chemistry, they must teach chemistry, and it generally takes the entire year to cover the ideas in the course. And this is neither bad nor good; it just is. Zooming out a bit in our analysis, it actually ends up being objectively good that there is some sort of benchmark for knowledge that all students must have. As mentioned in previous notes, if we desire an educated electorate which will select capable and appropriate leaders, each individual must have a baseline level of knowledge on which they can base their choices. In other words, it's in everybody's best interest that there aren't voters wandering around without any basic ideas about how the world around them works, from the functioning of their own bodies and the environment, to how their power is generated and how their cars run.

Here's the rub, though. If you ask someone at the education department, you'll also get the answer of "the tests" in response to why we have separate classes. The thing is, these are the people who can *decide* what these tests look like. Or when they happen. Or how integrated they are. So when the question of siloed knowledge or learning is brought up, the thing that underlies all that is really what the *assessments* look like, not what we expect students to know. There are myriad ways to teach chemistry, but these options are significantly narrowed if multiple-choice questions are the way you figure out how well the material was learned.

The question remains, however, of what a STEAM-ish, integrated test would look like. It could take the form of graduation-by-demonstration, or a comprehensive portfolio. Either of these choices (and there are others) would show growth (something that, in New York, our pre- and post-tests are supposed to show), as well as mastery. It would also give students the option to truly embody the interdisciplinary nature of the NGSS and other documents like it. No longer would students be answering questions on a test; rather, they'd be answering an actual question, and using all the tools – science, technology, engineering, art or math – necessary to answer it well. Imagine the leaps in comprehension that we could make when we roll in the application of knowledge to its acquisition.

Get involved with your state government or state science organizations so that you can be on the front lines of shaping the next generation of STEAM learning!

D.M.S.
May, 2018
Ithaca, NY

INVESTIGATING ALTERED BRAIN CONNECTIVITY AND THE EFFECT OF EXTERNAL RHYTHMIC CUES IN STUTTERERS

Mona Tong, Grade 12, Clarkstown North High School, New City, NY

ABSTRACT

Persistent developmental stuttering, a disorder affecting approximately 1% of adults worldwide, is characterized by disfluencies in speech production. The present study uses functional magnetic resonance imaging (fMRI) to conduct resting-state functional connectivity (FC) analyses, which help uncover how firing patterns between different brain regions are statistically correlated, and make it easier to compare these patterns between groups. FC was used in this study to identify differences between people who stutter (PWS) and people with normal speech (PNS), correlations between FC and stuttering severity, and FC differences between 'rhythmic' and 'normal' behavioral conditions to better understand the stuttering "rhythm effect," in which speaking in pace to an external, rhythmic beat enhances fluency in PWS. I found that PWS had stronger FC between right frontal and cerebellar regions compared to PNS, and I also classified two types of compensation - 'successful' and 'attempted'. The right orbitofrontal cortex (OFC) and anterior frontal operculum (aFO) likely displayed 'successful' compensation because FC to these regions had a negative correlation with severity, while the right dorsal inferior frontal gyrus pars opercularis (dIFo) likely displayed 'attempted' compensation since FC to it had a positive correlation with severity (Fig. 1). Moreover, there was evidence found indicating that rhythm induces fluency, perhaps eliminating the need for right frontal/cerebellar compensation, and that rhythm may normalize deficits in speech initiation/termination in PWS. Collectively, the results from this study contribute to our

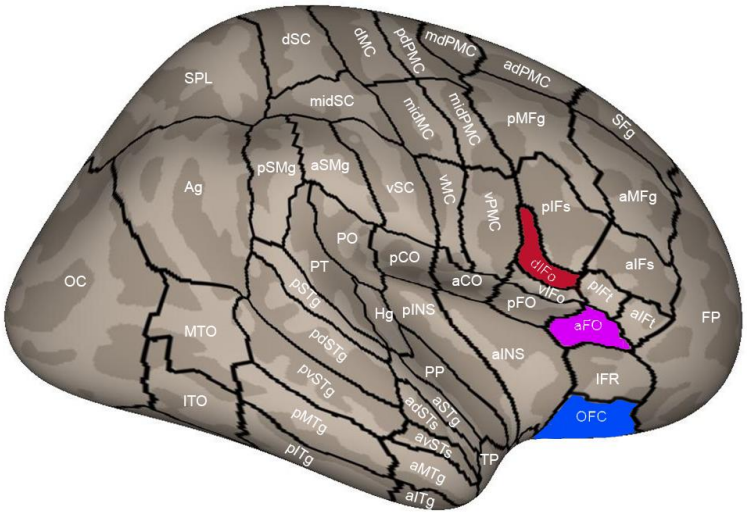

Figure 1. Right lateral view of the orbitofrontal cortex (OFC), anterior frontal operculum (aFO), and dorsal inferior frontal gyrus pars opercularis (dIFo).

understanding of the neural circuits underlying stuttering by using resting-state FC to both support past findings and introduce novel approaches and results.

INTRODUCTION

Persistent developmental stuttering is a neurological speech disorder that can severely affect a person's daily life by impeding their ability to verbally communicate. Characterized by involuntary repetitions, blocks, or prolongations of specific sounds or syllables in words, this disorder affects around 4-5% of children, but a majority of such children spontaneously recover. The remaining 1% who do not recover continue stuttering throughout adulthood (Bloodstein, 1995). However, due to the wide variability in the way stuttering manifests itself, its etiology remains unclear.

Various studies have shown that, in general, PWS have under-activations in left hemispheric speech areas but over-activations in motor areas and the right hemisphere (Fox et al., 1996; Braun et al., 1997; Chang, S.E. et al., 2009). Studies using resting-state FC, which find statistical associations between brain regions based on spontaneous fluctuations of the Blood Oxygen Level-Dependent (BOLD) fMRI signal, or fluctuations in deoxyhemoglobin content of blood at different neural firing levels, have not emerged until more recently to more accurately reveal core differences between PWS and PNS. Some previous studies involving FC have found that PWS have reduced FC between the left IFo and the bilateral premotor cortex, suggesting that PWS have a deficit in left hemispheric speech-motor control networks (Chang et al., 2011). In addition, dysfunction within the basal ganglia (BG) has been heavily implicated in stuttering, suggesting that stuttering may primarily be a motor disorder of speech (Alm, 2004; Max et al., 2004b) (Fig. 2). For example, PWS were shown to have reduced FC in the BG thalamo-cortical loop, indicating a possible deficit in self-initiated movement timing (Chang & Zhu, 2013). There are also studies investigating the compensatory mechanisms involved in stuttering. It has been shown that right frontal and cerebellar regions are overactive in PWS in comparison to PNS, suggesting these regions' involvement in taking on a greater speech production load to compensate for deficiencies in the left hemispheric speech network (Neumann et al., 2003; Preibisch et al., 2003; Brown et al., 2005; Kell et al., 2009; Lu et al., 2010).

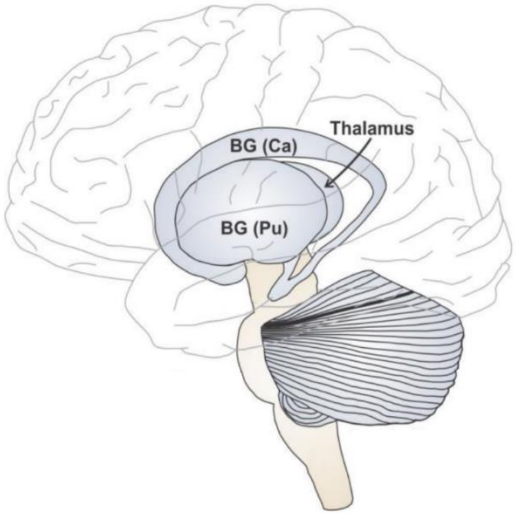

Figure 2. Left lateral view of basal ganglia subcortical structure.

It has been clearly and consistently shown, however, that PWS become considerably more fluent under certain fluency-inducing conditions, including metronome-timed speech,

choral speech, singing, masking, and transformed auditory feedback (Fox et al., 1996; Braun et al., 1997; Stager et al., 2003; Toyomura et al., 2011). Fox et al. (1996) compared neural activations between PWS and PNS under two conditions: normal reading aloud and choral reading. They found that the choral reading condition reduced and, in some cases, even eliminated, many of the motor region over-activations and auditory region under-activations present in the normal speech condition. In another study measuring regional cerebral blood flow (rCBF) under singing and metronome-timed speech conditions, both PWS and PNS exhibited increased bilateral auditory and motor activations. But the effects in activation was significantly greater for PWS than PNS in the left hemisphere (Stager et al., 2003). Toyomura et al. (2011) compared neural activation patterns of PWS and PNS under normal, choral reading, and metronome-timed speech conditions, and like Stager et al. (2003), found increased bilateral auditory activations in both PWS and PNS, but greater left hemispheric auditory activation in PWS than PNS, although this was based on uncorrected statistics. They also noticed that compared to the normal condition, BG activity increased for the metronome-timed speech condition but generally remained the same for the choral reading condition.

Of all the fluency-inducing conditions, it has been shown that metronome-timed speech and chorus reading are among the most effective, invoking at least a 90% reduction in stuttering (Andrews et al., 1982). However, there is evidence that rhythmic metronome-timed speech is an even stronger fluency-enhancing condition than chorus reading (Toyomura et al., 2011). Metronome-timed speech, in which people speak to the pace of a metronome, induces what is called the "rhythm effect" in PWS by providing external timing cues for each speech sound. These external timing cues are hypothesized to compensate for deficient internal timing cues of PWS likely within the BG, which projects output signals to the supplementary motor area (SMA), a region that plays a key role in internally-cued movements. (Alm, 2004). There is also evidence indicating that the rhythm effect does not require external pacing stimuli and that an internal generation of rhythm is just as effective in inducing fluency (Barber, 1940; Stager et al., 2003). All this suggests that stuttering is primarily a disorder involving the failure of the BG in producing effective timing cues for the initiation and termination of speech motor segments.

The goal of this study was to better understand the altered connectivity distinguishing PWS from PNS and those with less severe stutters from those with more severe stutters. I hypothesized that based on previous literature, there would be evidence of decreased FC in left hemispheric speech networks in PWS and increased FC in right hemispheric networks that may be forced to compensate for left hemispheric impairments. The goal also lies in analyzing the neural circuitries underlying the rhythm effect in stuttering, as no previous study has measured correlations between rhythmic speech and FC. Since stuttering involves dysfunction across multiple brain regions and systems, whole-brain FC analyses allow us to more holistically uncover novel findings about the neural circuitry underlying stuttering, and thus, hopefully advance treatment development for PWS in the future.

MATERIALS AND METHODS

Participants

Twelve adults who stutter (PWS; 4 female; age range: 19 - 58, mean age: 32.5) and nine adults who do not stutter (PNS; 4 female; age range: 21-44, mean age: 28.4) participated in this study. All participants were native English speakers.

Stuttering severity was assessed by a speech-language pathologist using the Stuttering Severity Instrument-4 (SSI-4). Stuttering severity was rated based on each participant's fluency and naturalness of speech during a reading passage, a conversation with the speech-language pathologist, and a phone call, in addition to the number of physical concomitants (e.g. head movements, facial grimaces) expressed during the session. In the SSI-4 assessment, both frequency of disfluencies and duration of stutters are converted to a scale from 2-18, and physical concomitants are converted to a scale from 0-20, for a total score range of 4-56. A lower score indicates less severe stuttering, while higher scores indicate more severe stuttering. Among the PWS in this study, scores ranged from 7-39 (very mild - very severe stutter), with a mean score of 23.2 (mild/moderate stutter).

Behavioral Session

The study is divided into 2 parts: 1 sound-booth behavioral session and 1 fMRI session. During the behavioral session, participants were asked to read aloud short sentences in one of two conditions: 'rhythmic' and 'normal'. There were 16 sentences in total, but one sentence, ‘the steady bat gave birth to pups’, appeared more frequently than the rest. During the 'rhythmic' condition, participants heard a series of short isochronous beats prior to viewing each sentence and were visually cued by the word “rhythmic” written in blue to read the sentence at the same rate that the beats were presented (i.e. each syllable aligning to each beat). The beats were only on before viewing the sentence and not while participants were speaking in order to eliminate potential confounds caused by auditory stimulation. During the 'normal' condition, participants heard the same isochronous series of beats before each sentence, but were visually cued by the word “normal” written in green to read the sentence at a normal rate and rhythm. These beats were presented during the ‘normal’ condition as well as during the ‘rhythmic’ condition in order to reduce any potential confounds.

In addition, the rate of each beat varied slightly from trial to trial, and participants were told to pay close attention to the varying rate, in order to have them pay closer attention to their task at hand. Participants were also shown how loud and how fast their speech was and were told to speak at a medium volume and a medium speed. Moreover, participants were shown how rhythmic their speech was, according to how well each syllable/vowel aligned to the beat. I then tallied the number of trials in each condition that included a disfluency. Two PWS were excluded from the disfluency analysis because their behavioral data either could not be located or was not properly saved in the correct file format to allow for analysis.

Image Acquisition

Each participant's brain was imaged at the Athinoula M. Martinos Center for Biomedical Imaging at Massachusetts General Hospital using a Siemens Magnetom Skyra 3-Tesla scanner, which allowed for fast structural and functional image data acquisition. Using the Magnetom Skyra, high-resolution T1 structural images were acquired (TR = 2530ms; TE = 1.69ms; TI = 1100ms; flip angle = 7 degrees; 1 x 1 x 1 mm^3 isotropic voxels; 256 x 256 matrix, 176 slices) for all participants, as well as 6 minutes of resting-state functional connectivity data (TR = 1120ms; TE = 30ms; 3 x 3 x 3 mm^3 voxel size). All of the neuroimaging data was collected from the same subjects who participated in the behavioral session of the study.

Data Processing

The CONN Functional Connectivity toolbox was used to preprocess and analyze whole-brain BOLD correlations and anti-correlations to brain networks. The preprocessing stage included motion correction, slice-timing correction, realignment, unwarping, ART outlier detection, segmentation, normalization, and smoothing with a Gaussian kernel. Measured stuttering severity scores and the numbers of disfluencies for both 'rhythmic' and 'normal' conditions were used as 2nd-level covariates in the analysis. I used Freesurfer (http://freesurfer.net) to map the anatomical landmarks (cortical parcellations and subcortical segmentations) of each subjects' brain using T-1 weighted structural images. The region of interests (ROIs) were then created (101 total) and mapped for each individual in functional space, based on the existing, publically-accessible Desikan-Killiany-Tourville (DKT) brain atlas (Klein & Tourville, 2012). I then conducted seed-to-voxel connectivity analyses measuring differences in regional brain association/FC strength between PWS and PNS, stuttering severity correlations, number of 'rhythmic' condition disfluencies correlations, and number of 'normal' condition disfluencies correlations.

RESULTS

Group Differences

Using the CONN Toolbox, I first measured the BOLD activity during resting-state fMRI sessions in PWS and PNS, in order to identify any fundamental differences in regional connectivity strength between the groups (Table 1). Under a voxel-wise threshold of $p<0.001$ and a cluster-corrected threshold of p-FDR<0.05, PWS had greater FC than PNS between the left planum temporale (PT) and the right OFC, left putamen, and left accumbens, as well as between the right ventral inferior frontal gyrus pars opercularis (vIFo) and left cerebellum lobule 6. PWS also had greater FC than PNS between the right posterior superior temporal gyrus (STG) and the left cerebellum lobule 6, 8, crus 1 and crus 2 and vermis 6, 7, and 8. Meanwhile, PNS had greater FC between the left pre-SMA and the right thalamus and right hippocampus.

Seed	Region with Peak FC	Cluster Size	Coordinates in MNI	T-Value
Stutterers > Controls				
L. PT	R. Orbitofrontal Cortex	71	14, 12, -16	-7.06
	L. Putamen	49	-10, 4, -12	-6.81
	L. Accumbens	49	-10, 4, -12	-6.81
R. pSTG	Vermis 6, 7, 8	86	0, -66, 24	-6.60
	L. Cerebellum Crus 1, Crus 2	86	0, -66, 24	-6.60
	L. Cerebellum 6, 8	86	0, -66, 24	-6.60
R. vlFo	L. Cerebellum 6	41	-26, -60, -18	-5.75
Controls > Stutterers				
L. pre-SMA	R. Thalamus	234	18, -34, 6	8.16
	R. Hippocampus	234	18, -34, 6	8.16

Table 1. Regional Data.

Stuttering Severity Correlations

Next, I measured how regional FC correlated to stuttering symptom severity by using stuttering severity scores (SSI-4) from the PWS group as 2nd-level covariates in CONN Toolbox (Table 2). Revealed correlations between FC and stuttering severity not only help reinforce findings from the 'Group Differences', but may also shed some light on novel FC patterns in PWS. Continuing to use the voxel-wise threshold of $p<0.001$ and cluster-corrected threshold of p-FDR<0.05, I found a negative correlation between stuttering severity and FC from the left pre-SMA to the bilateral precentral (motor cortex) and postcentral (somatosensory cortex) gyrus, as well as from the left ventral motor cortex to the right motor cortex. I also found a negative correlation between severity and FC from the right OFC to the left cerebellum lobule 8 and 7b, and from the right anterior frontal operculum (FO) to the right cerebellum lobule 6 and crus 1. There was also a positive correlation between stuttering severity and FC between the right dIFo and the bilateral cerebellum lobule 6 and crus 1, and right cerebellum lobule 8.

Seed	Region with Peak FC	Cluster Size	Coordinates in MNI	T-Value
Positive Correlation				
R. dlFo	R. Cerebellum 8	73	6, -52, -66	9.53
	L. Cerebellum 6, Crus 1	45	-34, -50, -36	9.94
	R. Cerebellum 6, Crus 1	29	40, -44, -36	6.63
Negative Correlation				
L. pre-SMA	R. Precentral Gyrus	61	42, -12, 44	-9.03
	L. Precentral Gyrus	32	-22, -26, 54	-7.50
	R. Postcentral Gyrus	61	42, -12, 44	-9.03
	L. Postcentral Gyrus	32	-22, -26, 54	-7.50
L. vMC	R. Precentral Gyrus	32	34, -14, 62	-6.89
R. OFC	L. Cerebellum 8, 7b	36	-38, -62, -54	-6.96
R. aFO	R. Cerebellum 6, Crus 1	45	36, -66, -22	-8.80

Table 2. Regional Correlation data.

Number of Disfluencies per Condition Correlations

In addition to measuring the relationship between FC and stuttering severity, I also measured the relationship between FC and the number of disfluencies detected in PWS during the behavioral session for both 'rhythmic' and 'normal' speaking conditions (Table 3). The usage of FC in any way to analyze the "rhythm effect" in stuttering has never been done before, thus, this investigation of the relationship between resting-state FC and number of disfluencies per speaking condition is novel as well. I found such a relationship between resting state FC and disfluencies in 'rhythmic' and 'normal' conditions highly probable because I found that among PWS in the behavioral session, the number of disfluencies when speaking rhythmically was significantly lower than the number of disfluencies when speaking normally (Fig. 3).

Seed	Region with Peak FC	Cluster Size	Coordinates in MNI	T-Value
Number of Disfluencies in the 'Normal' Condition				
Positive Correlation				
L. pSTG	R. Orbitofrontal Cortex	50	2, 38, -30	9.77
R. vlFo	R. Orbitofrontal Cortex	16	20, 34, -14	6.88
R. vMC	R. Cerebellum 6	35	22, -54, -26	15.05
Negative Correlation				
L. Caudate	L. Precentral Gyrus	16	-50, -2, 16	-8.28
	L. Postcentral Gyrus	27	-14, -46, 66	-9.39
	R. Postcentral Gyrus	16	22, -38, 58	-9.32
L. Pallidum	L. Precentral Gyrus	27	-56, -4, 10	-8.05
	L. Postcentral Gyrus	10	-60, -8, 16	-12.62
Number of Disfluencies in the 'Rhythmic' Condition				
None matching seed-to-voxel results from the 'Normal' Condition for both positive and negative correlations				

Table 3. Rhythmic and normal correlation data.

Using the same voxel-wise threshold of $p<0.001$ and cluster-corrected threshold of p-FDR<0.05, I found a positive correlation between number of disfluencies in the 'normal' condition and FC from the right OFC to the left posterior STG and right vIFo, as well as from the right ventral motor cortex to the right cerebellum lobule 6 in PWS. However, there was no significant correlation between number of disfluencies in PWS in the 'rhythmic' condition and FC between those same regions. Moreover, I found a negative correlation between number of disfluencies in the 'normal' condition and FC between the left caudate and bilateral somatosensory cortex and left motor cortex, as well as between the left pallidum and left motor and somatosensory cortex in PWS. However, again there was no significant correlation between number of disfluencies in PWS in the 'rhythmic' condition and FC between those same regions.

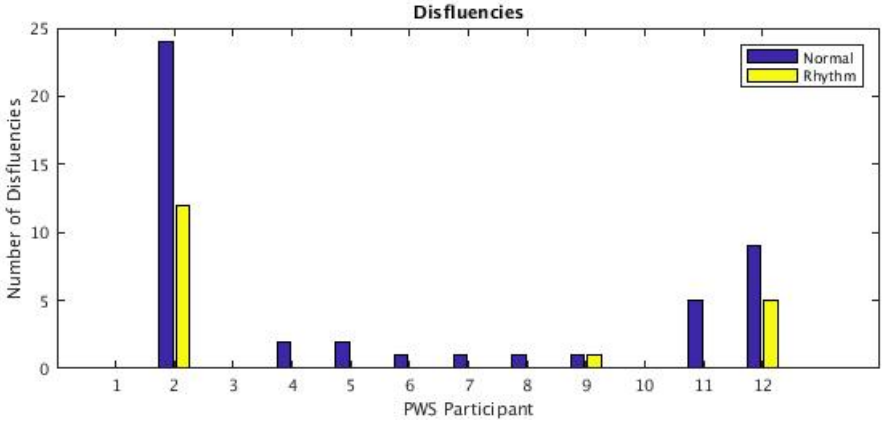

Figure 3. Number of disfluencies by participant.

DISCUSSION

Previous studies have demonstrated the potential involvement of right frontal and cerebellar areas in compensating for dysfunctional left hemispheric speech networks in PWS (Neumann et al., 2003; Preibisch et al., 2003; Brown et al., 2005; Kell et al., 2009; Lu et al., 2010; Chang et al., 2011). In addition, it has been suggested that the best compensation occurs between two functionally-connected cortical and subcortical compensatory networks (i.e. OFC-cerebellum) (Sitek et al., 2016). My findings support both theories, but seem to also suggest that there are two different types of compensation: 'successful' and 'attempted'. A negative correlation between stuttering severity and FC would represent 'successful' compensation, in that people who stutter less severely are able to more successfully compensate than people who stutter more severely. A positive correlation between severity and FC would represent 'attempted' compensation in PWS, in that these regions attempt to correct for errors that arise due to the primary disturbance. For example, in the DIVA model, the feedback control map would be forced into action to correct auditory and somatosensory errors detected when PWS speak (Tourville & Guenther, 2011). So as errors increase, these 'attempted' compensatory regions must increasingly kick in to correct for them. It was found that PWS consistently had greater FC between right frontal areas as well as cerebellar areas, supporting my hypothesis. However, when correlated with stuttering symptom severity, it was shown that while the FC between the right OFC and left cerebellum, and between the right aFO and right cerebellum displayed a negative correlation with severity, the FC between the right dIFo and bilateral cerebellum displayed a positive correlation with severity. Thus, such evidence suggests that the right OFC and right aFO are involved in 'successful' compensation of stuttering, while the right dIFo is associated with 'attempted' compensation in PWS.

My interpretation is in keeping with prior findings, which has found that right FO activation negatively correlates with stuttering severity, and has therefore been implicated in successful compensation (Preibisch et al., 2003; Neumann et al., 2003). In addition, the right OFC has been associated with stuttering symptom avoidance and its activation has also been shown to negatively correlate with stuttering severity in past studies (Sowman et al., 2012; Kell et al., 2009). However, a previous FC study by Yang et al. (2016) has found a positive

correlation between stuttering severity and FC between the right cerebellum lobule 6 and right IFo, which, according to my interpretation, implies that as more errors are detected, more FC between these 'attempted' compensatory regions is needed to correct for such errors. These consistent results from the literature strengthen my claim for the existence of two different types of compensation in PWS.

In addition, the pre-SMA is functionally involved in speech-planning and articulatory processing, and is implicated to be heavily connected to the cortico-BG planning loop (Lee et al., 2012). Thus, the finding that PWS have deficient FC between the left pre-SMA and right thalamus likely indicates a potential deficit in the speech-planning aspect of the BG-mediated planning loop, which serves as an 'input gate' enabling the selection and initiation of the appropriate upcoming speech motor programs in the GODIVA model (Bohland et al., 2010). This further supports the theory that a problem in stuttering lies in the failure to select for and initiate forthcoming speech segments in time. Moreover, it was found that PWS have greater FC from the left PT to the left putamen than PNS. Functionally, auditory areas project input into the BG to monitor auditory feedback for sequencing, so greater FC between auditory and BG regions would likely indicate that PWS excessively rely on auditory feedback to perhaps compensate for their dysfunctional left hemispheric speech networks (Civier et al., 2010). Additionally, a decrease in excessive left putamen activity has been shown to be necessary for successful treatment in PWS, further lending support to my findings and helping to reinforce the goal of future treatment to decreasing left putamen activity (Ingham et al., 2013).

My results also showed a negative correlation between stuttering severity and FC between the left pre-SMA and bilateral motor and somatosensory cortices, which are functionally involved in controlling movements of speech articulators and other sensory and motor aspects of speech production (Tourville & Guenther, 2011). This reveals a potential dissociation between speech planning and speech-motor execution components that gets worse in PWS as stuttering severity increases. A negative correlation between stuttering severity and FC between the left ventral motor cortex and the region of the dorsal motor cortex associated with respiration was also found, hinting at a possible disturbance between breathing, articulation, and speech-motor components during stuttering (Van Riper, 1936; Bloodstein, 1995; Guenther et al., 2006).

Moreover, speaking in pace to a rhythmic beat has consistently shown to create a fluency-inducing "rhythm effect" in PWS, in which it is likely that the rhythmic cues compensate for impaired internal timing (Alm, 2004). The cause of this deficient internal timing in PWS likely lies in the BG, which is functionally involved in internal rhythm generation during speech motor control; impairment in the BG would therefore cause difficulty in fluently producing sequential words (Taniwaki et al., 2006). Evidence of such BG impairment was present, as there was a negative correlation in PWS between number of disfluencies in the 'normal' condition and FC between BG regions and the motor and somatosensory cortices. However, there was no detected correlation between number of disfluencies in the 'rhythmic' condition and FC between these same regions. This may indicate that rhythm has the effect of

temporarily normalizing BG and motor/somatosensory function in PWS, and thus, the timely initiation, termination, and speech-motor execution of sounds. This supports previous studies that found evidence of rhythmic speaking raising the normally low BG activity of PWS to the same level as that of PNS (Toyomura et al., 2011; Stager et al., 2003; Braun et al., 1997). Stager et al. (2003) also saw similarly increased-activation in the ventral precentral gyrus (motor cortex) in PWS under fluency-evoking conditions. Therefore, perhaps the presence of rhythmic cues does not necessarily compensate for deficient internal timing cues and speech-motor execution in PWS, but instead, temporarily corrects for it.

There was also evidence found that potentially suggested that the speaking in pace to rhythmic stimulus normalizes over-activation of compensatory regions in PWS. My results demonstrated a positive correlation between number of disfluencies for the 'normal' condition and FC to right frontal and cerebellar 'compensatory' regions. However, no correlation between number of disfluencies for the 'rhythmic' condition and FC to these same compensatory regions was seen, suggesting that these regions needed to be recruited for compensation under the 'normal' condition, but perhaps their compensatory roles were no longer needed during the 'rhythmic' condition as fluency improved. This interpretation is supported by a study conducted by Fox et al. (1996), which found that cerebellar activations were doubled in PWS compared to PNS under normal conditions, but such cerebellar over-activations were eliminated in PWS under the induced-fluency choral reading condition. Thus, it is likely that the "rhythm effect" temporarily normalizes BG and speech-motor execution function in PWS (as noted before), which in turn, significantly improves fluency and perhaps eliminates the need for further right frontal and cerebellar compensation.

CONCLUSIONS

This study continues and furthers ongoing research investigating brain functional connectivity differences in people who stutter (PWS) compared to people with normal speech (PNS). PWS displayed greater functional connectivity (FC) to right frontal and cerebellar brain regions in comparison to PNS, providing evidence of compensation for stuttering. After correlating stuttering severity with FC, I was able to classify two different types of compensation -- 'successful' and 'attempted'. The former displayed a negative correlation between severity and FC while the latter showed a positive correlation. I concluded that the right orbitofrontal cortex (OFC) and anterior frontal operculum (aFO) are associated with 'successful' compensation, while the right dorsal inferior frontal gyrus pars opercularis (dIFo) is associated with 'attempted' compensation. Evidence further suggests that PWS have impairments in the cortico-basal ganglia (BG) planning loop, which affects their ability to select and initiate speech motor programs. PWS perhaps also excessively rely on auditory feedback and have dissociations between speech-motor articulation and respiration components during speech production.

This study also introduces a novel approach to studying the "rhythm effect" in stuttering through comparing 'normal' and 'rhythmic' conditions. This was done by correlating the number

of disfluencies to resting-state FC for each condition. Speaking rhythmically in pace to an isochronous beat significantly lowered disfluencies in comparison to speaking normally by perhaps normalizing BG and motor/somatosensory function, and thus, likely eliminating the need for right frontal and cerebellar compensation since fluency improved so drastically. Primarily, my results indicate the necessity of developing treatments in the future that improve BG function, since it is clear, through this study and previous studies, that metronome-timed speech is effective in improving fluency because it likely has the capability of normalizing the BG in PWS.

Future research on this topic would benefit from a larger sample size to increase the level of confidence in results, as there were only a total of 21 participants (12 PWS; 9 PNS). Moreover, this study only focused on resting-state FC with number of disfluencies per condition as a covariate, which made some of the results more difficult to interpret and maybe less reliable. Future studies investigating the "rhythm effect" should perhaps analyze functional scans during 'normal' and 'rhythmic' conditions and directly compare the differences in FC between the conditions in order to further validate and raise confidence in these results.

REFERENCES

Alm, P.A. (2004). Stuttering and the basal ganglia circuits: A critical review of possible relations. *Journal of Communication Disorders, 37*(4), 325-369.

Andrews, G., Howie, P., Dozsa, M., & Guitar, B. (1982). Stuttering: Speech pattern characteristics under fluency-inducing conditions. *Journal of Speech and Hearing Research, 25,* 208– 216.

Barber, V. (1940). Studies in the psychology of stuttering, XVI: rhythm as a distraction in stuttering. *Journal of Speech and Hearing Disorders 5,* 29–42.

Bloodstein O. (1995) A Handbook of Stuttering 5 Ed. San Diego, California: Singular Publishing Group.

Bohland, J.W., Bullock, D., & Guenther, F.H. (2010). Neural representations and mechanisms for the performance of simple speech sequences. *Journal of Cognitive Neuroscience, 22*(7), 1504–1529.

Braun, A.R., Varga, M., Stager, S., Schulz, G., Selbie, S., Maisog, J.M., Carson, R.E., & Ludlow,
C.L. (1997). Altered patterns of cerebral activity during speech and language production in developmental stuttering. An H2(15)O positron emission tomography study. *Brain, 120,* 761–784.

Brown, S., Ingham, R.J., Ingham, J.C., Laird, A.R., & Fox, P.T. (2005). Stuttered and fluent speech production: an ALE meta-analysis of functional neuroimaging studies. *Human Brain Mapp. 25,* 105–117.

Chang, S.-E., Kenney, M.K., Loucks, T.M., & Ludlow, C.L. (2009). Brain activation

abnormalities during speech and non-speech in stuttering speakers. *Neuroimage, 46*(1), 201-212.

Chang, S.-E., Horwitz, B., Ostuni, J., Reynolds, R., & Ludlow, C.L. (2011). Evidence of left inferior frontal–premotor structural and functional connectivity deficits in adults who stutter. *Cerebral Cortex, 21*(11), 2507–2518.

Chang, S.-E., & Zhu, D.C. (2013). Neural network connectivity differences in children who stutter. *Brain, 136,* 3709–3726.

Civier, O., Tasko, S.M., & Guenther, F.H. (2010). Overreliance on auditory feedback may lead to sound/syllable repetitions: simulations of stuttering and fluency-inducing conditions with a neural model of speech production. *Journal of Fluency Disorders, 35*(3), 246–279.

Fox, P. T., Ingham, R.J., Ingham, J.C., Hirsch, T.B., Downs, J.H., Martin, C., Jerabek, P., Glass, T., & Lancaster, J.L. (1996). A PET study of the neural systems of stuttering. *Nature, 382*(6587), 158-162.

Guenther, F.H., Ghosh, S.S., & Tourville, J.A. (2006). Neural modeling and imaging of the cortical interactions underlying syllable production. *Brain and Language, 96*(3), 280-301.

Ingham, R.J., Fox, P., Ingham, J., Xiong, J., Zamarripa, F., Hardies, L., & Lancaster, J. (2004). Brain correlates of stuttering and syllable production. *Journal of Speech Language and Hearing Research, 47*(2), 321-341.

Ingham, R.J., Wang, Y., Ingham, J.C., Bothe, A.K., & Grafton, S.T. (2013). Regional brain activity change predicts responsiveness to treatment for stuttering in adults. *Brain and Language, 127*(3), 510-519.

Kell, C.A., Neumann, K., Kriegstein, K.V., Posenenske, C., Gudenberg, A.W., Euler, H., & Giraud, A. (2009). How the brain repairs stuttering. *Brain, 132*(10), 2747-2760.

Klein, A., & Tourville, J. (2012). 101 labeled brain images and a consistent human cortical labeling protocol. *Frontiers in Neuroscience,* 6:171.

Lee, Y-S., Turkeltaub, P., Granger, R., & Raizada, R.D.S. (2012). Categorical speech processing in broca's area: An fMRI study using multivariate pattern-based analysis. *Journal of Neuroscience, 32*(11), 3942-3948.

Lu, C., Peng, D., Chen, C., Ning, N., Ding, G., Li, K., Yang, Y., & Lin, C. (2010). Altered effective connectivity and anomalous anatomy in the basal ganglia-thalamocortical circuit of stuttering speakers. *Cortex, 46,* 49–67.

Max L., Guenther F.H., Gracco V.L., Ghosh S.S., & Wallace M.E. (2004b). Unstable or insufficiently activated internal models and feedback-biased motor control as sources of dysfluency: A theoretical model of stuttering. *Contemporary Issues in Communication Science and Disorders, 31,* 105–122.

Neumann, K., Euler, H.A., von Gudenberg, A.W., Giraud, A.-L., Lanfermann, H., Gall, V., & Preibisch, C. (2003). The nature and treatment of stuttering as revealed by fMRI: A within- and between-group comparison. *Journal of Fluency Disorders, 28,* 381–410.

Preibisch, C., Neumann, K., Raab, P., Euler, H.A., Gudenberg, A.W., Lanfermann, H., &

Giraud, A. (2003). Evidence for compensation for stuttering by the right frontal operculum. *NeuroImage, 20*(2), 1356-1364.

Sitek, K.R., Cai, S., Beal, D.S., Perkell, J.S., Guenther, F.H., & Ghosh, S.S. (2016). Decreased cerebellar-orbitofrontal connectivity correlates with stuttering severity: whole-brain functional and structural connectivity associations with persistent developmental stuttering. *Frontiers in Human Neuroscience, 10,* 190.

Sommer, M., Koch, M.A., Paulus, W., Weiller, C., & Büchel, C. (2002). Disconnection of speech-relevant brain areas in persistent developmental stuttering. *The Lancet, 360*(9330), 380-383.

Sowman P.F., Crain S., Harrison E., & Johnson B.W. (2012). Reduced activation of left orbitofrontal cortex precedes blocked vocalization: a magnetoencephalographic study. *Journal of Fluency Disorders, 37,* 359–365.

Stager, S.V., Jeffries, K.J., & Braun, A.R. (2003). Common features of fluency-evoking conditions studied in stuttering subjects and controls: an H(2)15O PET study. *Journal of Fluency Disorders, 28,* 319–336.

Taniwaki, T., Okayama, A., Yoshiura, T., Togao, O., Nakamura, Y., Yamasaki, T., Ogata, K., Shigeto, H., Ohyagi, Y., Kira, J., & Tobimatsu, S. (2006). Functional network of the basal ganglia and cerebellar motor loops in vivo: Different activation patterns between self-initiated and externally triggered movements. *Neuroimage, 31,* 745–753.

Tourville, J.A., & Guenther, F.H. (2011). The DIVA model: A neural theory of speech acquisition and production. *Language and Cognitive Processes, 26*(7), 952–981.

Toyomura, A., Fujii, T., & Kuriki, S. (2011). Effect of external auditory pacing on the neural activity of stuttering speakers. *Neuroimage, 57*(4), 1507-1516.

Van Riper, C. (1936). Study of the thoracic breathing of stutterers during expectancy and Occurrence of stuttering spasm. *Journal of Speech Disorders, 1*, 61-72.

Yang, Y., Jia, F., Siok, W.T., & Tan, L.H. (2016). Altered functional connectivity in persistent developmental stuttering. *Scientific Reports, 6*(1).

TO WHAT EXTENT IS MECHANICAL LIFE OF A CONTACTOR RELATED TO A DETERIORATION IN ITS PERFORMANCE OVER A PERIOD OF TIME.

Rajavi Mishra, Class 11 IB, Step By Step School, Noida, India

ABSTRACT

This paper presents an analysis of the visual features and the testing results for specific parameters of three alternating current (AC) contactors rated 220 volts 50 Hz 25 ampere. While one contactor has completed its mechanical life, the other two are on their initial stages - wherein one belongs to a normal range while the other belongs to an economy range i.e. a range of cheaper contactors. Visual inspection emphasizes on the present appearance of each of the contactors' components. Furthermore, the results from functional, mechanical and secureness tests have been compiled and analyzed in the light of the research aim. The specific parameters tested were pick up and drop out voltage, overtravel and full travel, connection and disconnection time and consumption. The paper attempts to observe and analyze the differences in the aforementioned features in the three contactors and hence trace why and how a contactors performance deteriorates as it ages.

INTRODUCTION

Before a contactor, or any other electrical application for that matter, is deemed qualified for usage, there are specific tests and inspection methods that are designed in order to approve the application for usage. In this paper, these designed tests and visual inspection will be used to trace the deterioration in the performance of the contactor. Contactors are electromechanical switches of different voltage and current readings, used in electrical circuits which require the process of making(pick) and breaking(drop) [1]. For instance, these may include starting and stopping of a motor, switching control systems for energy distribution and transmission, industrial machinery, electrically controlling light installation etc. Similar to a relay, the process of switching a contactor is controlled by a lower power level circuit in order to control the switched circuit with a higher power level [2]. Therefore contactors are for higher current ratings as compared to a relay. There are various parameters that can be tested in order to understand a contactor's performance.

For mechanical testing, no load (current) is provided to the contactor because it only involves making and breaking of contacts by energizing the coil and completing the circuit. This process is controlled by the hour meter. Parameters to understand the mechanical life contactors

include Pick Up voltage, Drop Out voltage, consumption, contact resistance, opening time (time at which contacts break), closing time (time at which contacts make), Overtravel and Full travel. For Electrical life testing, the aim is to provide the load to measure the electrical life in terms of operations. Under this, the electrical endurance of a contactor is tested in accordance with the guidelines AC-4 utilization category. Due to this, six times the rated current is flowed during making and breaking of contactors.

Similarly, for thermal testing, temperature rise tests are done on the terminals and coils. Firstly, the thermal current flows into one terminal which then forms loops on the rest of the terminals except for the last one which goes back to the power supply, completing the circuit. A thermocouple is used to sense the temperature on the terminals. After the terminals, the coil is energized. The ambient temperature is subtracted from the final, stable temperature of the coil to understand the temperature rise in coils. A formula can be used to calculate the temperature rise in the coil:

$$\textbf{Temperature Rise} = R_1 \div R_2 \,[234.5 + T_1] - 234.5$$

Where,
T_1 - Initial Temperature
T_2 - Final Ambient Temperature
R_1 - Winding hot Resistance
R_2 - Winding cold Resistance
[234.5 is the extrapolated temperature for copper at zero resistance]

These thermal tests can also be carried out inside a humidity chamber where field conditions can be recreated.

Next, a secureness test can be conducted in order to know about the weight that the contactor can bear by attaching weights to it. Furthermore, secureness can also be tested by providing a high voltage to the contactors. This is imperative in detecting a dielectric failure wherein a contactor has already failed although the silver discs on the contacts have not yet welded. This occurs when a charge buildup exceeds the electrical limit or dielectric strength of a material [3]. During this test, 2.5kV or more can be provided from pole to pole or pole to base of the contactor for 1 min. If an error is detected or anticipated, it can be concluded that a dielectric failure has occurred.

For this study, only test results for secureness, Pick Up voltage, Drop Out voltage, consumption, contact resistance, opening time (time at which contacts make), closing time (time at which contacts break), Overtravel and full travel, and visual inspection will be considered for analysis.

DESIGN AND VISUAL INSPECTION

Design

All three four pole contactors- Economy range and Normal range on initial stage, and Normal range which has crossed its mechanical life , rated 220 V 50 Hz 25 A, have the same design. Through visual inspection, it was understood that economy and normal range on initial stage were similar, whereas the one which has crossed its mechanical life differs from the two. The contactor was opened up and each and every part or component was inspected. All three contactors consist of a base made up of Technyl, and black Polyamide on which is an E shaped fixed laminated electromagnet or core, made up of cold rolled non-oriented steel. It is placed on and surrounded by a rubber damper on two sides in order to reduce noise and humming as a contactor makes and breaks. In the middle, a coil of copper wire, surrounded by insulating tape, bobbin and an ultramide coil shroud, is fixed and on the sides of the electromagnet aluminium shading rings are fixed. Then at the top is a laminated moving E-shaped electromagnet or core, also made up of cold rolled oriented steel. Both the electromagnets have been laminated to prevent heat loss because steel itself being a conductor of electricity, changing magnetic flux will induce eddy currents due to which extra heat loss takes place. Hence it is attached to a black carrier on the top which consists of moving contacts of brass sheet and a silver disc at the end. These contacts are fixed inside a carrier using small pole springs. This is covered by an ultramide archood which consists of fixed contacts made of brass sheet and silver discs on the tips. These contacts are attached using screws which are further covered by Akulon shrouds This top part, consisting of archood, carrier and moving magnet, is joined to the bottom part of base, fixed electromagnet and coil by using a return spring.

When the coil is energized, current flowing through the conductor, copper wire, generates a magnetic flux around it. Cutting of flux lines by the core or magnetic flux linkage induces an EMF and hence a current in the fixed core or electromagnet due to which the moving electromagnet at the top gets attracted to fixed core. The presence of shading rings on the half side of the electromagnet is highly significant for making and breaking of the contacts. If slip rings were not present, then a complete AC cycle would drop to zero twice which would lead to constant vibration which is not required for efficient working. Therefore, shading rings are used which have an AC cycle that lags with the AC cycle of the primary coil. When, in the primary coil, the rate of decreasing or increasing of AC is maximum, i.e. when it is dropping to zero, then the AC in shading rings is maximum. When the rate slows down for primary i.e. when it is at peak, then the cycle drops to zero for shading rings. When the primary coil is energized then a current is induced in shading ring which produces a 90 degree out of phase magnetic field such that the flux is never zero (Figure 2.11). The inner side of the core is energized by the magnetic flux of the coil while the outer side is energized by shading ring.

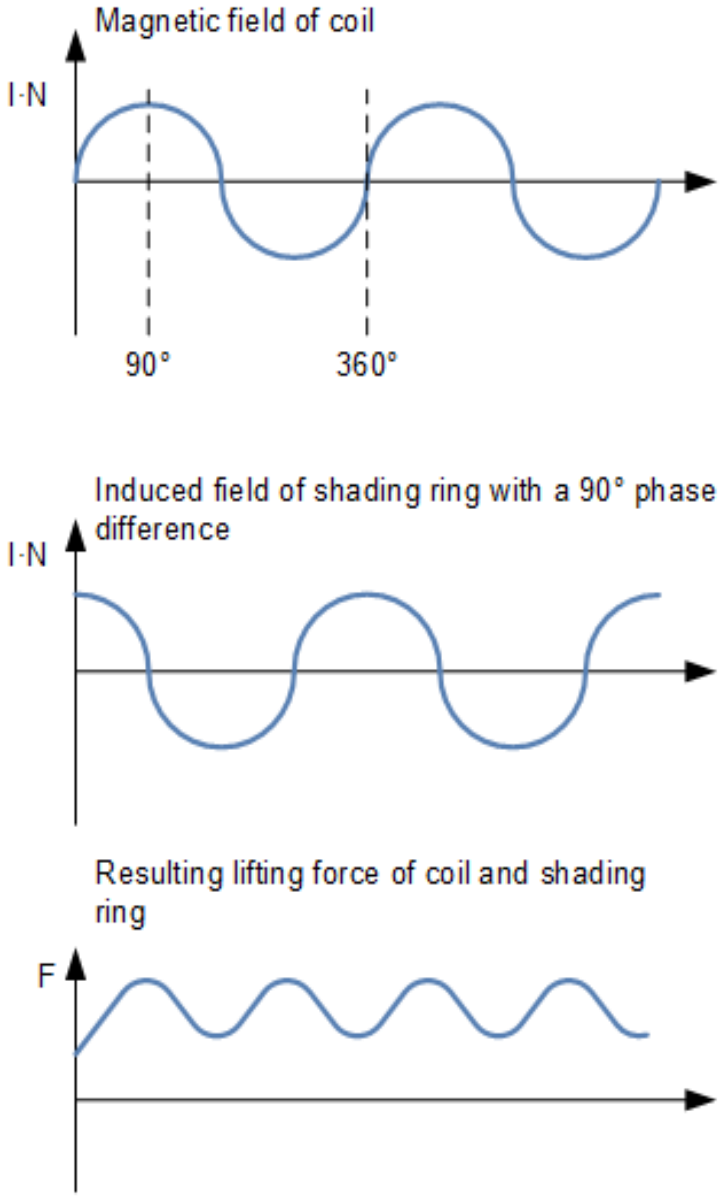

Figure 2.11: AC Cycle of the Primary Coil

Visual Inspection

After the visual inspection, it was observed that the contactor which had completed its mechanical life had undergone some changes in its parts. The magnet had deteriorated with time (Figure 2.21) and the air space between the fixed and the moving electromagnet had increased from 0.03 to 0.04 mm and it was very slightly deformed which can be explained by the constant striking of the moving magnet on the surface of the fixed magnet. There were carbon deposits on various parts of the contactor. The contacts were oxidized and the return spring had loosened (Figure 2.22), hence resulting a lower tensile strength. There was a very small crack on the shading ring but they were not significant. More significant cracks and even breaking of shading

rings (Figure 2.23) were observed in the shading rings of those contactors which had failed before completing their mechanical life which usually occurs during assembly of parts leading to a development of cracks not visible through naked eyes of a factory worker on the assembly line. But this was the case observed in those contactors of same rating (220v 50Hz 25 amperes) which had not completed their mechanical life. In some of these, burning of the coil was also seen because in mechanical life testing the coil is energized, hence a high voltage results in the continuous heating. The bobbin was also melted. However, the extent to which it was seen in the one which had completed mechanical life was higher than those which hadn't. Because of such changes in the structure, the contactor which had completed its mechanical life was deemed unqualified for any further usage as opposed to those which were in their initial stage of usage (both economy range and normal).

Figure 2.21: Deteriorated Magnet

Figure 2.22. Oxidized contacts.

Figure 2.23: Deteriorated shading rings

TESTING

Total Travel and Over Travel

Total travel is the total distance travelled by the carrier for making the contacts and coming back to break the contacts. The formula is as follows:

Total Travel = Overtravel + Arc Gap

Overtravel is the distance travelled by the carrier more than what is necessary to perform the task of making and breaking. After the arc gap is covered, overtravel creates an extra force that is exerted on the pole springs. On the other hand, the Arc gap occurs due to the spring which returns to its original shape and position in the absence of current and hence a magnetic field. Total travel and Overtravel was measured using a travel Gauge. Firstly, as the carrier was picked and the making of contacts took place, the needle was inserted and set on zero. The carrier was dropped or the breaking of the contacts took place which gave the reading for Total travel. For Overtravel, after taking the value of the Total travel, two wires ending with a conductor were made to touch the terminal screws, such that when the contacts touched with no extra pressure on the pole springs, the LED on the panel glowed thus giving the over travel. This was done for all four poles of the three contactors rated as 220 volts 50 Hz 25 ampere.

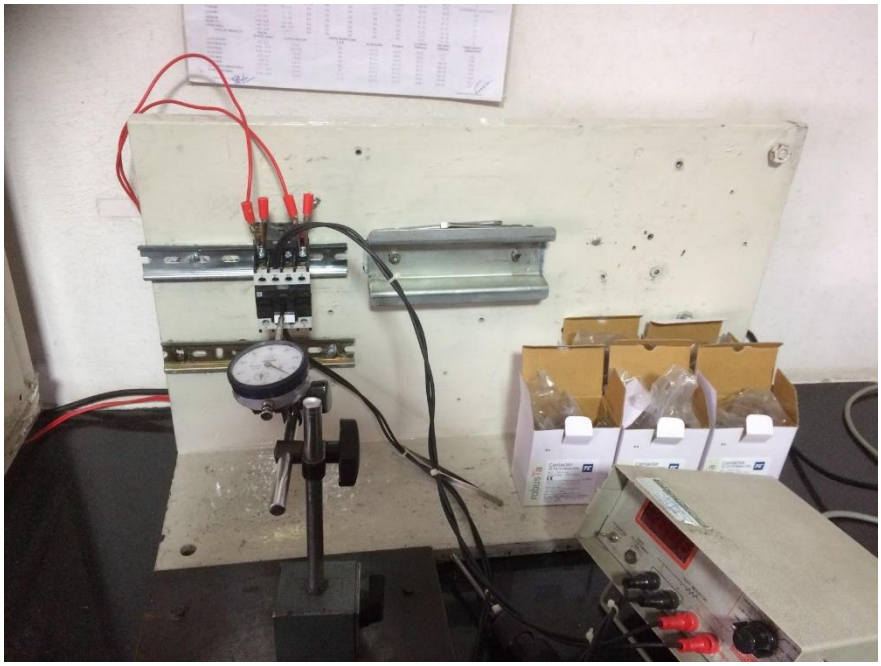

Figure 3.1: Travel Gauge setup for Overtravel and Total Travel Calculation

RESULTS AND OBSERVATIONS

Parameters	**TC1D25004 Complete Mechanical Life**	**TC1D25004 Initial Stage of Usage Parameters**	**TC1D25004E - Economy Range Initial Stage Parameters**
Full Travel (mm)	6.28	6.35	6.2
Overtravel L1T1 (mm)	1.90	1.88	1.84

Overtravel L2T2 (mm)	1.58	1.53	1.46
Overtravel L3T3 (mm)	1.44	1.38	1.32
Overtravel L4T4 (mm)	1.62	1.56	1.24

Table 3.111: Full Travel and Overtravel Data Compiled

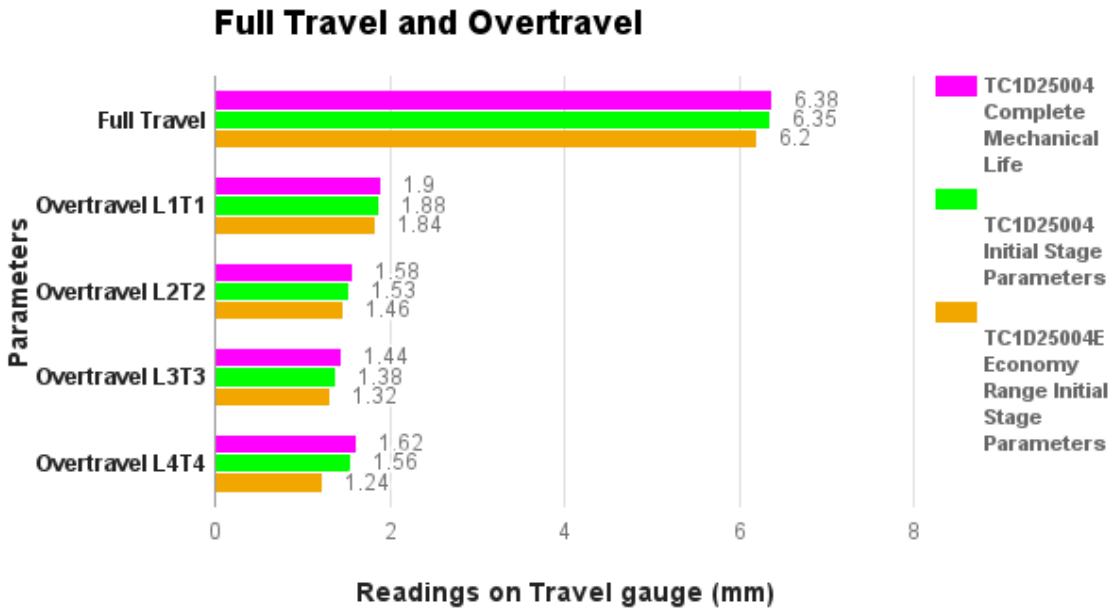

Figure 3.112: Graphical Display of Data from Table 3.11.

ANALYSIS

From Figure 3.12, it can be observed that while the Full travel and the overtravel were maximum for the contactor which had completed its mechanical life, both parameters were minimum for the economy range contactor on its initial stage of usage. When reasons were traced down, it was observed that due to an increase in the air gap from 0.03 to 0.04 mm, the distance had increased. The continuous striking of the moving electromagnet on the fixed magnet had created this air gap. Since the contactor (whose mechanical life was completed) had witnessed 16 million operations of pick and drop, this air gap and hence, an increase in the magnitude of overtravel and total travel are justified. On the other hand, the overtravel and the total travel were lowest for the economy range contactor due to a lower volume of silver (calculated using Vernier calipers) used in the silver contacts.

Pick-Up and Drop Out Voltage, and Consumption

Pick-up and drop out voltage are the voltages at which the contacts make and break respectively. The pick-up, drop out, and consumption (in amperes) were recorded by looking at the panel of AC power supply.

Contactor	**Pick Up Voltage (V)**	**Drop Out Voltage (V)**	**Consumption(mA)**
TC1D25004 Complete Mechanical Life	**147**	**90**	**37.1**
TC1D25004 Initial Stage of Usage Parameter	**153**	**95**	**38.8**
TC1D25004E - Economy Range Initial Stage Parameters	**150**	**92**	**37.9**

Table 3.211: Full Travel and Overtravel Data Compiled

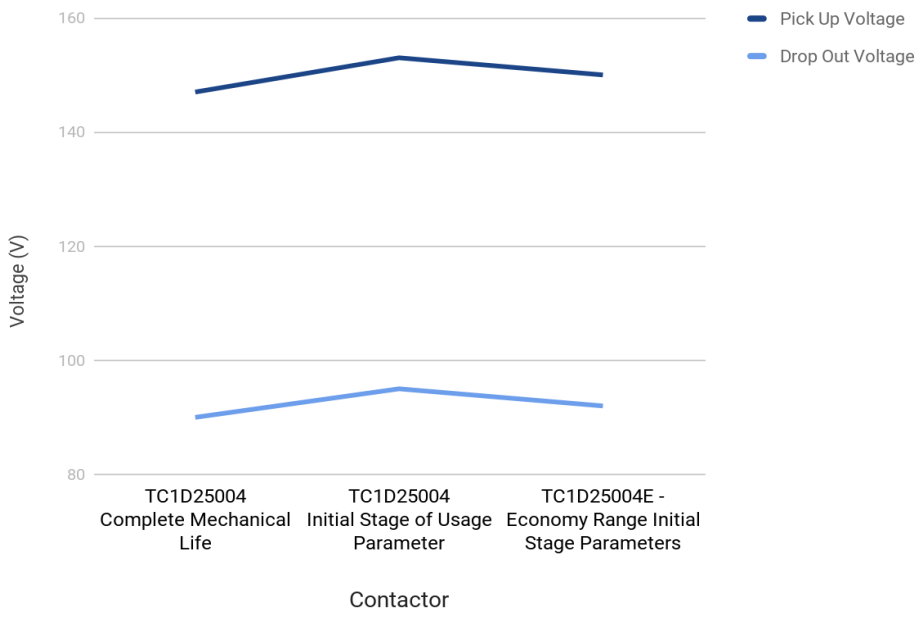

Figure 3.212: Graphical Display of Data from Table 3.21.

ANALYSIS

Figure 3.22 shows that the pick up voltage is almost within band, almost similar for contactors on initial stage of usage belonging to normal and economy range. But the contactor whose mechanical life is completed, the pick-up and drop out voltage are low. When the contactor (whose mechanical life was completed) was inspected, it was observed that its return

spring was more stretched and had lower tensile strength and lower spring load as compared to the return spring of the contactor which was still in early stage of use. Due to this, the making and breaking of contacts took place earlier for the contactor whose mechanical life was completed. This excessive stretching occurred in the return spring due to repetitive making and breaking of the contactor for about 16 million operations. Furthermore, since all of the contactors have a rated current of 25 amperes, therefore the consumption lies in the range, with not much of a difference.

CLOSING AND OPENING TIME

Closing and Opening Time which tells about the time taken to pick and drop respectively, which can be recorded using a CRO Oscilloscope. Closing time is basically the time from when the supply for energizing the coil is turned on to the time at which the contacts make. On the other hand, the opening time is the time from which the supply was turned off to the time at which the contacts actually break.

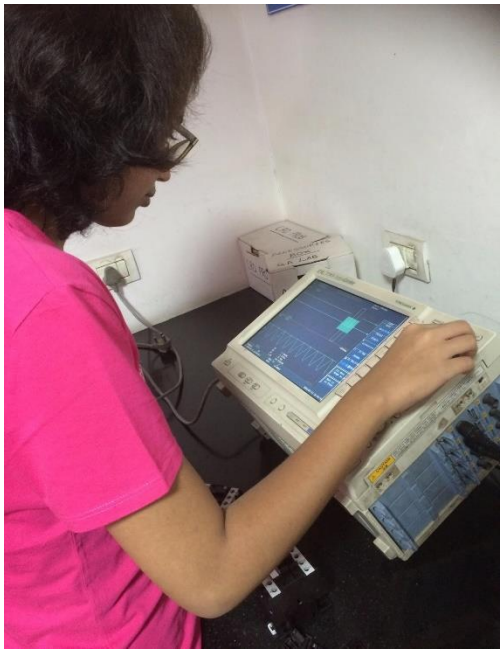

Figure 3.31: Observing and Measuring the Closing and the Opening Time using CRO Oscilloscope

RESULTS AND OBSERVATIONS

Contactor	**Closing Time (milliseconds) (Dark Blue)**	**Opening Time (milliseconds) (Light Blue)**
TC1D25004 Complete Mechanical Life	17	12

TC1D25004 Initial Stage of Usage Parameter	18	11
TC1D25004E - Economy Range Initial Stage Parameters	18	10

Table 3.311: Full Travel and Overtravel Data Compiled

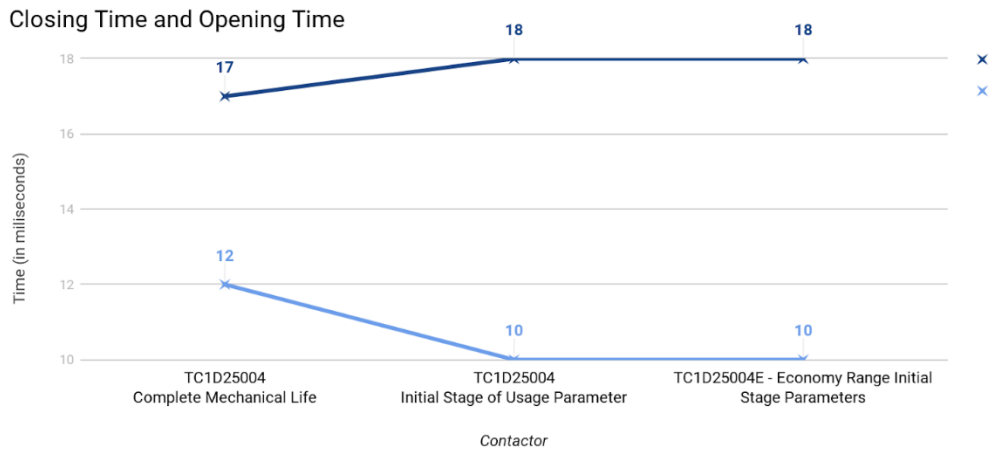

Figure 3.312: Graphical Display of Data from Table 3.21.

ANALYSIS

On one hand, contactors in their initial stage of usage from both normal and economy range showed similar results. However, there was an increase in the opening time in the contactor which had completed its mechanical life. This can be due to a decreased drop out voltage in the contactor. Furthermore, there was a decrease in the closing time which can be explained by a decreased pick up voltage. These results can be seen because of stretch of spring, a decrease in spring load and lower tensile strength. A link can also be made to Hooke's Law, according to which 'force needed to extend or compress a spring is proportional to that distance' ((Robert Hooke, "De Potentia Restitutiva, or of Spring. Explaining the Power of Springing Bodies", London, 1678.)). This proportionality presents us with the spring constant and hence the stiffness of the spring.

$$F \propto x$$

F = kx, where k is the spring constant that determines the stiffness of the spring

When the coil has an approximately zero value magnetic flux, the spring force exceeds the magnetic closing force between the magnets causing the contacts to break for that portion of the cycle. This depends upon the spring constant of the return spring used to open the contactor**.**

CONCLUSIONS

In this paper, by examining the observations and analyzing the testing results, it can be stated that if a contactor reaches its mechanical life, then it undergoes certain changes in its appearance and its parameters which can be tested and are dependent on various factors like spring constant, area of air gap, the extent to which contacts oxidize, volume of silver etc. These changes contribute to a deterioration in the performance of the aging contactor and hence classifies a contactor as unqualified for any further usage. For further experimentation, other tests mentioned in the introduction can be done to understand the extent to which the central claim is true.

Through this paper I was successfully able to analyze that, in addition to visual changes, various functional parameters changed as well. For instance, the pick up and drop out voltage decreased, opening time increased, closing time decreased, consumption almost remained the same with respect to its rated ampere reading, and overtravel and final travel increased for the contactor which had completed its mechanical life. According to the study, this is how a contactor changes in its due course of ageing, contributing to a deterioration in its performance.

ACKNOLWEDGEMENTS

I would like to highly thank C&S Electric Noida Plant for allowing me to carry out my research in the testing lab. Furthermore, I would like to acknowledge Dr. Raj Singh and Ms. Neha Choudhary for their assistance at C&S Electric.

REFERENCES

1) J.-R. R. Ruiz, A. Garcia, J. Cusidó, and M. Delgado, "Dynamic model for AC and DC contactors – simulation and experimental validation", Simulation Modeling Practice and Theory, vol. 19, pp. 1918-1932, 2011

2) T. Croft and W. Summers (ed), " American Electricians' Handbook, Eleventh Edition, McGraw Hill", New York (1987) ISBN 0-07-013932-6 page 7-124

3) Hong, Alice (2000). Dielectric Strength of Air". The Physics Factbook.

4) Robert Hooke, "De Potentia Restitutiva, or of Spring. Explaining the Power of Springing Bodies", London, 1678.

ECONOMY MATTERS: MISLABELING AND *PSEUDOMONAS* CONTAMINATION OF SALMON SOLD IN SEATTLE AND NEW YORK

Naomi Alam, Grade 11, Manhattan Center for Science and Mathematics, New York, NY; Sofia Kashtelyan, Grade 11, High School of American Studies, New York, NY and Christine Marizzi, Cold Spring Harbor Laboratory, DNA Learning Center, Harlem DNA Lab, New York, NY

ABSTRACT

Here we outline how DNA barcoding empowers citizen scientists to make taxonomic identifications of food items based on diagnostic genes. Our research team tested 12 samples of fresh and smoked salmon ranging from a fish market in the Pacific coast to local grocery stores and restaurants on the Atlantic coasts in order to test the validity of proper fish labeling in grocery stores, fish markets and restaurants by utilizing DNA barcoding. Furthermore, we tested each piece of salmon for the presence of parasites such as Japanese broad tapeworms and bacteria. Starting with generic primers for species identification we then used more specific primers to increase our resolution at the species level. The result of our research was that salmon mislabeling is neither prevalent in NYC nor Seattle; in fact, only one of our samples was inaccurately labeled. We could not detect DNA associated with tapeworms, however, we found *Pseudomonas* species in all of our samples, including *Pseudomonas fluorescence* that can be potentially harmful for vulnerable immunocompromised patients.

INTRODUCTION

DNA barcoding has many practical applications including identification of fraud in consumer products (3). Like a unique pattern of bars in a universal product code (UPC) identifies each consumer product, a short "DNA barcode" (about 500 nucleotides in length) is a unique pattern of DNA sequence that can potentially identify each species (3). The technique allows for quick and accurate species identification using only minimal amounts of tissue samples taken from any organism at any developmental phase – ideal for testing fish fillets where morphological identification using taxonomic keys is difficult to nearly impossible.

In our project we focused on the mislabeling and contamination of salmon products sold in New York City (NYC), New York and Seattle, Washington. We also searched for the existence of parasites such as Japanese broad tapeworms in our samples, as recent Centers for Disease Control and Prevention (CDC) studies reported that wild pink salmon caught in Alaska had been infected by this parasite. Four species of Pacific salmon have been identified as the principal sources of human infection and the popularity of eating raw fish may be responsible for the increased number of infections outside the area where Pacific salmon naturally occurs (1). It has been reported that salmon is mislabeled 43% of the time in the off-season and 7% in the peak

of the fishing season, including farmed Atlantic salmon that has been sold as wild-caught product for a higher price (2). We hypothesized that the more expensive wild salmon products have a higher misidentification rate because they might be substituted by a different and cheaper species, which will lead to an increase in mislabeling due to low seasonal availability of the fish. Furthermore, we hypothesize that restaurants will serve more mislabeled fish in comparison to supermarkets. Restaurants purchase fish in bulk from vendors and are not required to provide consumers with species-specific labels, thus increasing the chance of seafood fraud. To identify our samples down to the species level we followed the DNA barcoding workflow as outlined at www.dnabarcoding101.org.

MATERIALS AND METHODS

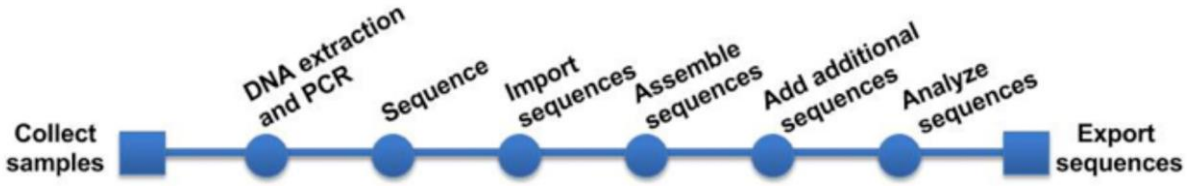

Figure 1. DNA barcoding workflow.

Our project workflow is depicted in Figure 1. We obtained 12 samples of salmon from 2 locations - NYC and Seattle. In NYC we obtained 8 samples in the Bronx and 1 in Manhattan (9 total). In Seattle all three samples came from the same location (Figure 2). The samples we collected ranged in price (2.75 to 15.79 $ per sample) and type (50 % fresh/ 25% frozen/ 25% smoked.) Additionally, 50% of samples were purchased in grocery stores while the other 50% came from restaurants. The samples were collected during salmon's off-season, between February and April. Salmon is in season May through September (http://www.alaska.org/advice/best-time-to-fish-in-alaska).

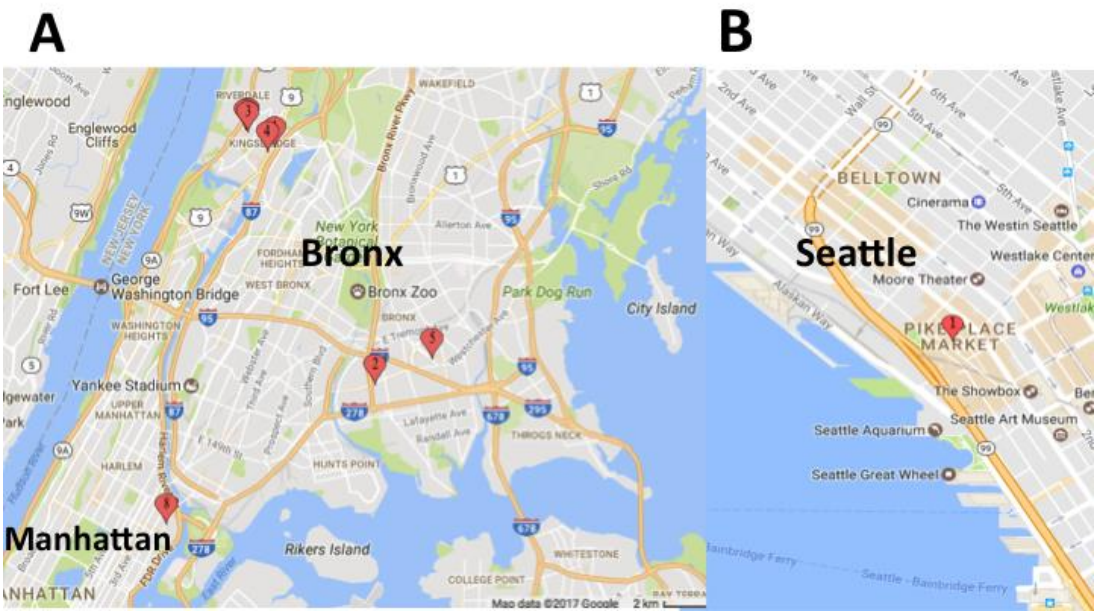

Figure 2. Locations of the samples collected. Maps of NYC (A) and Seattle (B) indicating where samples were obtained. The figure was prepared based on Google Maps data and edited by Naomi Alam.

Following the standard DNA barcoding protocol we extracted genomic DNA from sample tissues using the silica DNA extraction method. We performed Polymerase Chain Reaction (PCR) to amplify the cCytochrome *c* oxidase subunit 1 *(CO1)* barcode region for fish and parasites, and tested and compared two different primer sets for fish-specific DNA barcoding (4,5). In addition, we employed PCR to amplify the 16S rRNA gene region for bacteria using universal and *Pseudomonas* genus specific primers (6,7) (all primer sequences are listed in Table 1). To streamline sequencing all primers contained identical M13F(-21) and M13R(-27) "tails".

Primer Name	Sequence 5' -> 3' (with M13 tags)	DNALC Name	Reference
Fish			
VF2_t1-M13F	TGTAAAACGACGGCCAGTCAACCAACCACAAAGACATTGGCAC	Fish Cocktail	Ivanova et al. 2007 (4)
FishF2_t1-M13F	TGTAAAACGACGGCCAGTCGACTAATCATAAAGATATCGGCAC	Fish Cocktail	Ivanova et al. 2007 (4)
FishR2_t1-M13R	CAGGAAACAGCTATGACACTTCAGGGTGACCGAAGAATCAGAA	Fish Cocktail	Ivanova et al. 2007 (4)
FR1d_t1-M13R	CAGGAAACAGCTATGACACCTCAGGGTGTCCGAARAAYCARAA	Fish Cocktail	Ivanova et al. 2007 (4)
FISHCOILBC_ts-M13F	TGTAAAACGACGGCCAGTCAACYAATCAYAAAGATATYGGCAC	FishBOL	Baldwin et al. 2009 (5)
FISHCOIHBC_ts-M13R	CAGGAAACAGCTATGACACTTCYGGGTGRCCRAARAATCA	FishBOL	Baldwin et al. 2009 (5)
Invertebrate			
mlCOIint-M13F	TGTAAAACGACGGCCAGTGGWACWGGWTGAACWGTWTAYCCYCC	Updated DMI	Leray et al. 2013 (7)
mlCOIintR-M13R	CAGGAAACAGCTATGACGGRGGRTASACSGTTCASCCSGTSCC	Updated DMI	Leray et al. 2013 (7)
Bacteria			
Bac1492Runiv-M13R	CAGGAAACAGCTATGACCGGTTACCTTGTTACGACTT	16S rRNA Bacteria	Jiang et al. 2006 (7)
Bac27Funiv-M13F	TGTAAAACGACGGCCAGTAGAGTTTGGATCMTGGCTCAG	16S rRNA Bacteria	Jiang et al. 2006 (7)
PA-GS-M13F	TGTAAAACGACGGCCAGTGACGGGTGAGTAATGCCTA	Pseudomonas Specific	Spilker et al. 2004 (6)
PA-GS-M13R	CAGGAAACAGCTATGACCACTGGTGTTCCTTCCTATA	Pseudomonas Specific	Spilker et al. 2004 (6)

Table 1. Primer sets used in this study.

PCR success was verified through gel-electrophoresis (Figure 3). Samples that showed sufficient amplification were sent off for PCR cleanup using ExoSAP-IT, and bidirectional Sanger cycle- sequencing using Big Dye on an Applied Biosystems ABI 3730xl DNA Analyzer

at Genewiz (South Plainfield, NJ). on an ABI 3730 Automated Sequencer through Genewiz Inc. After obtaining the sequences we used the open-access *DNA Subway* (www.dnasubway.org) interface to assemble, trim and edit the sequences, then aligned the sequences using the MUltiple Sequence Comparison by Log- Expectation program (MUSCLE). Results were verified through independent search on NCBI's Basic Local Alignment Search Tool, nucleotide work suite (BLASTn; https://blast.ncbi.nlm.nih.gov/Blast.cgi?PAGE_TYPE=BlastSearch) and The Barcode of Life Datasystems (BOLD; http://www.boldsystems.org/). For each sample the top BLAST result was determined using the highest percent identity score. In the event of a tie between two identity scores, the lowest e-value was used as a deciding-factor. If there were identical e-values and identity scores for multiple species, samples were only identified to the genus level.

RESULTS

DNA extraction and PCR and sequencing

Of the 12 samples we extracted, the majority of samples amplified and sequenced for both fish *COI* and 16S rDNA (Figure 3). Fresh samples amplified with a success rate of 90%, which is significantly better than frozen and smoked samples (66%). We saw that the FishBOL primer set had higher efficacy in both amplification and species discrimination compared to standard Fish cocktail primers (63% vs. 37% amplification success rate, respectively). Interestingly, standard Fish cocktail primers amplified weakly and returned several sequencing results that matched *Pseudomonas* species. While it has been reported that "universal" DNA barcoding primers can anneal to bacterial species in error (8), we verified this result with an additional PCR using 16S rDNA and *Pseudomonas* genus specific primers. During this project the CDC announced that salmon being sold for human consumption were found to be contaminated with tapeworm parasites. We therefore tested whether our fish samples contained parasites by amplifying our samples with invertebrate-specific *COI* primers. None of the samples showed a clearly positive PCR amplification with invertebrate specific *COI* primers, there was a weak amplification in one sample (sample "D") that didn't return any sequencing results.

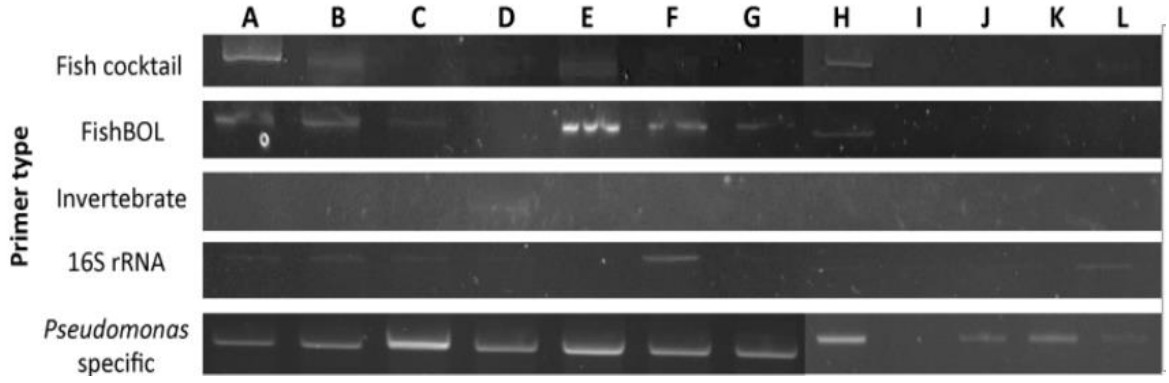

Figure 3. The bands show the efficacy of primers in DNA amplification and sequencing.

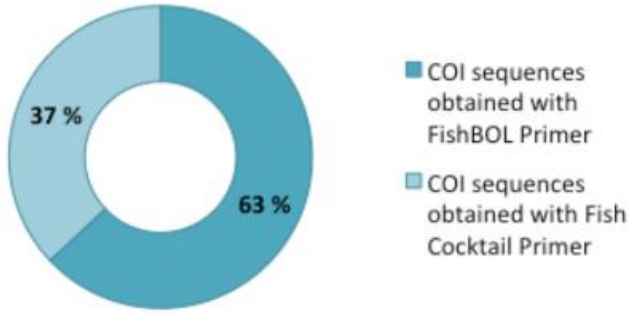

Figure 4. The efficacy of primers in DNA amplification and sequencing.

Species Identification

Eight out of 12 salmon samples were identified to the species level (Table 2); and represented four different salmon species: *Oncorhynchus nerka* (sample A; 8%), *Oncorhynchus tshawytscha* (sample H; 8%), *Oncorhynchus keta* (sample I; 8%) and *Salmo salar* (samples B,C,E,F,G; 41%). The 16S rDNA sequences generated with *Pseudomonas* specific primers allowed to identify 4 *Pseudomonas* species in our salmon samples (Table 3): *P. fragi, P. fluorescence, P. psychrophila,* and *P. parafulva*, based on 100% of similarity with other reference sequences of those species included in NCBI GenBank. We found that 58 % of fish samples contained *Pseudomonas* species, but GenBank was unable to resolve it down to the species level, therefore they were only classified as *Pseudomonas* sp. During this project the CDC announced that salmon being sold for human consumption were found to be contaminated with tapeworm parasites. We therefore tested whether our fish samples contained parasites by amplifying our samples with invertebrate-specific *COI* primers. None of the samples showed a clearly positive PCR amplification with invertebrate specific *COI* primers, there was a weak amplification in one sample (sample "D"), that didn't return any sequencing results. As conclusion we considered all samples parasite free.

Sample	Origin	Description	Price/Sample	Fish sp. Per Label	*COI* Barcoding ID	Common Name
A	Grocery Store	Frozen Fillet	$15.79	Sockeye Salmon	*Oncorhynchus nerka*	Sockeye Salmon
B*	Grocery Store	Frozen Fillet	$7.99	Red (Sockeye) Salmon	*Salmo salar**	Atlantic Salmon*
C	Grocery Store	Fresh Fillet	$9.99	Atlantic Salmon	*Salmo salar*	Atlantic Salmon
D	Grocery Store	Fresh Fillet	$9.99	Not declared	No sequence obtained	No sequence obtained
E	Grocery Store	Fresh Fillet	$10	Farmed Salmon	*Salmo salar*	Atlantic Salmon
F	Restaurant	Sushi	$2.75	Atlantic Salmon	*Salmo salar*	Atlantic Salmon
G	Restaurant	Sashimi	$3	Scottish Salmon	*Salmo salar*	Atlantic Salmon
H	Restaurant	Sashimi	$4	King Salmon	*Oncorhynchus tshawytscha*	King Salmon
I	Fish Market	Smoked Salmon	$5.59	Keta Salmon	*Oncorhynchus keta*	Keta Salmon
J	Fish Market	Smoked Salmon	$11.98	Keta Salmon	*Oncorhynchus keta*	Keta Salmon
K	Fish Market	Smoked Salmon	$11	Keta Salmon	No sequence obtained	No sequence obtained
L	Grocery Store	Frozen Fillet	$5.49	Canadian Salmon	No sequence obtained	No sequence obtained

Table 2. Sample analysis and fish species with their common names and scientific names.
* Indicates a substitution.

Sample	*Pseudomonas Spp.*	Characteristics	Pathogenesis reported for humans
A	*Pseudomonas sp.*		Depending on species
B	*P. fragi*	Opportunistic microbiota [9] Food Spoilage [10]	None
C	*P. parafulva*		None
D	*P. parafulva*		None
E	*P. fluorescens*	Opportunistic pathogen in fish [11] Seafood Spoilage [10]	Immunocompromised patients [12]
F	*Pseudomonas sp.*		Depending on species
G	*Pseudomonas sp.*		Depending on species
H	*Pseudomonas sp.*		Depending on species
I	*Pseudomonas sp.*		Depending on species
J	*Pseudomonas sp.*		Depending on species
K	*P. fluorescens*	Opportunistic pathogen in fish [11] Seafood Spoilage [10]	Immunocompromised patients [12]
L	*P. psychrophila*		None

Table 3. Characteristics of the *Pseudomonas* species detected in commercial fish and potential risk for humans.

DISCUSSION AND CONCLUSIONS

We conclude that salmon mislabeling and therefore marketplace substitutions were not as prevalent as expected. Out of the 12 samples only one was mislabeled: one grocery store sold Atlantic salmon (*Salmo salar*) as the more expensive Pacific Red salmon (*Oncorhynchus nerka).* We conclude that out of the 12 samples one was mislabeled. One grocery store sold Atlantic salmon as Pacific Red salmon. We were unable to detect parasite DNA via PCR and therefore we considered all samples parasite free.

However, we identified bacteria of the *Pseudomonas* genus in all samples tested. This is not surprising, as the microflora that spoils fresh, ice-stored fish consists largely of *Pseudomonas* sp. (9,10,11). Bacteria from the *Pseudomonas* genus cause psychotrophic spoilage and do not survive heat processing, so their presence in processed food suggest post process contamination through biofilms on equipment (9,10). Although we did not find the most dangerous species of *Pseudomonas* for humans, *P. aeruginosa*, the *P. fluorescence* species found in our study could be potentially harmful for vulnerable or immunocompromised consumers. This is due to the capacity of *Pseudeomona.s fluorescence* to adhere to nerves, and it was reported to have caused outbreaks in oncology patients (12). While PCR is rapid and sensitive, it does not distinguish living from dead bacteria. *Pseudomonas* sp. are considered a health hazard for consumers only when their number exceeds 10^{6}- 10^{7} CFU/g of product (9,10). Suggestions for further research include additional testing using Standard Plate Count or fluorescence-based techniques to measure the count of total viable microorganisms in the salmon samples.

ACKNOLWDGEMENTS

This project was supported by the *Urban Barcode Research Program,* funded by the Pinkerton Foundation. We thank reviewers for their constructive comments. We thank Melissa Lee, Alison Cucco and Jenna Dorey (DNA Learning Center, Cold Spring Harbor Laboratory) for their helpful assistance.

REFERENCES

(1) https://wwwnc.cdc.gov/eid/article/23/2/16-1026_article. Accessed December 11th 2016.

(2) http://usa.oceana.org/press-releases/oceana-reveals-mislabeling-americas-favorite-fish-salmon. Accessed December 11th 2016.

(3) Hebert P.D.N., Gregory T.R. The promise of DNA barcoding for taxonomy. *Systematic Biology* 2005;54: 852–9.

(4) Ivanova NV., Zemlak TS, Hanner RH, Hebert PDN. Universal primer cocktails for fish DNA barcoding. *Molecular Ecology Notes*. 2007;7: 544–548.

(5) Baldwin CC, Mounts JH, Smith DG, Weigt LA. 2009. Genetic identification and color descriptions of early life-history stages of Belizean *Phaeoptyx* and *Astrapogon* (Teleostei: Apogonidae) comments on identification of adult *Phaeoptyx*. *Zootaxa* 2008:1 – 22.

(6) Spilker, T.; Coenye, T.; Vandamme, P. and LiPuma, J.J. PCR -based assay for differentiation of *Pseudomonas aeruginosa* from other *Pseudomonas* species recovered from cystic fibrosis patients. *Journal of Clinical Microbiology*. 2004 42(5): 2074-2079.

(7) www.dnabarcoding101.org

(8) Siddall ME, Fontanella FM, Watson SC, Kvist S, Erséus C. Barcoding bamboozled by bacteria: Convergence to metazoan mitochondrial primer targets by marine microbes. *Systematic Biology*. 2009. pp. 445–451.

(9) Gram, L.; Huss, H.H. Fresh and Processed Fish and Shellfish. In *The Microbiological Safety and Quality of Foods*; Lund, B.M., Baird-Parker, A.C., Gould, G,W., Eds.; Chapman and Hall: London, UK, 2000; pp. 472-506.

(10) Food Microbiology: An Introduction, Third Edition. ASM Press, 2012.

(11) Bruno, D.W.; Ellis, A.E. Salmonid Disease Management. *Development in Aquacultures and Fisheries Science.* 1996, 29, 729-824.

(12) Hseuh, P.R.; Teng, L.J.; Pan, H.J.; Chen, Y.C.; Sun, C.C.; Ho, S.W.; Luh, K.T. Outbreak of *Pseudomonas fluorescens* bacteremia among oncology patients. *Journal of Clinical Microbiologyo*,gt 1998, 36, 2914-2917.